Rev.Adv.Mater.Sci. 8 (2004) 101-106

CHARACTERIZATION OF CLEAVED SURFACES OF A MONOPHOSPHATE TUNGSTEN BRONZE

H. Guyot [1], N. Motta[2], E. Placidi [3] and H. Balaska[1,4]

[1]CNRS-LEPES, BP 166, 38240 Grenoble Cédex, France
[2] Dipartimento di Fisica, Universita di Roma Tre, Via della Vasca Navale 84, I-00146 Roma, Italy
[3] Dipartimento di Fisica, Universita di Roma Tor Vergata, Via della Ricerca Scientifica 1, I-00133 Roma, Italy
[4] University of Skikda, BP 26, Skikda, Algeria

Received: October 19, 2004

Abstract. [001] surfaces of $P_4W_8O_{32}$ obtained by cleavage in UHV are analyzed at room temperature by UPS, LEED and STM. Two types of facets are revealed. The type I shows periodic parameters very close to the parameters of the bulk unit cell. It corresponds to a relaxed (1x1) surface, and the surface defects may produce a (3x1) reconstruction. The type II facets show a periodicity of 7.45 E, that is the distance between two second neighboring tungsten sites and corresponds to facets parallel $(001)_p$, the dense planes of the perovskite-like WO_6 octahedra slabs. This parameter reflects also the width of the steps ending the WO_6 octahedra slabs.

1.INTRODUCTION

The phosphate tungsten bronzes are a new family of metallic oxides that slightly differs from the well-known family of the sodium tungsten bronzes, due to a presence of PO_4 tetrahedra [1]. While Na_xWO_3 has a distorted perovskite crystallographic structure, the monophosphate tungsten bronzes (MPTB) are built with infinite slabs of WO_6 octahedra, connected by double planes of PO_4 tetrahedra, which make the structure anisotropic. The MPTB, of generic formula $(PO_2)_4(WO_3)_{2m}$, with *m* ranging from 4 to 14, are metallic and show different transitions at low temperature towards modulated structures [2]. For small *m*, the transitions have been attributed to charge density wave instabilities. The *m* = 7 bronze shows in addition a superconducting transition [3-6].

The metallic character of the MPTB results from the presence of W5d electrons filling the conduction band, with a concentration of 2/*m* electrons per unit cell. The first element of the MPTB family, $P_4W_8O_{32}$, exhibits two electronic transitions at 80 and 52K. The modulation of the crystallographic structure below 80K, the transport properties and spectroscopic properties clearly demonstrate that the upper transition is originated by an incommensurate charge density wave instability with a [0.33, 0.295, 0] *q*-vector [7-9].

The shape of the Fermi surface plays a key role in the charge density wave transition. Quasi-cylindrical Fermi surface showing a large nesting area is necessary to achieve such a transition. Angle resolved photoemission experiments performed on (001) cleaved surface have evidenced the metallic nature of the bronze, determined the band structure and revealed the shape of the Fermi surface with an large nesting in the [0.33, 0.295, 0] direction [1-3].

The photoemission technique is nevertheless very sensitive to the nature of the top surface of the sample. Any roughness produced by the cleavage, any natural or controlled surface reconstruction may deeply alter the electronic structure of the surface and therefore hides the bulk band structure or the bulk Fermi surface. For that reason, ARPES mea-

Corresponding author: H. Guyot, e-mal: guyot@grenoble.cnrs.fr

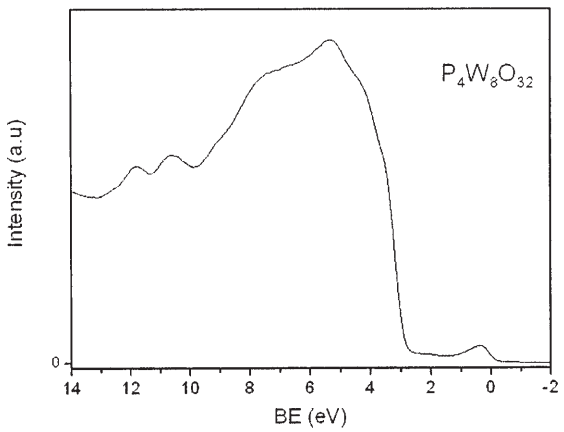

Fig. 1. EDC curve recorded at normal emission in $P_4W_8O_{32}$ on a freshly cleaved (001) surface.

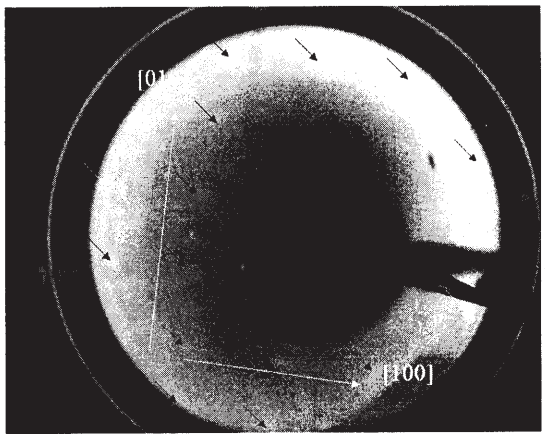

Fig. 2. LEED pattern (at 49 eV) of a $P_4W_8O_{32}$ single crystal cleaved parallel to the (001) plane. The electron beam (5 μA) reaches the entire crystal (2 x 2 mm^2). The weak contrasted pattern disappears after about 1 min of electron bombardment, due to a rapid surface deterioration.

surements have been performed on untreated surfaces of cleaved single crystals. We present a characterization of clean surfaces of $P_4W_8O_{32}$, obtained by cleaving single crystals parallel to (001).

2.EXPERIMENTAL

Single crystals of $P_4W_8O_{32}$ were grown as platelets by vapor phase transport technique. The stoichiometry was controlled by energy dispersive spectroscopy (EDS). The crystals were oriented using natural edges of the platelets, and glued between a copper sample holder and a vertical post. After having introduced the sample in the UHV chamber, the cleavage is done by removing the post from the top of the sample. The quality of the surface is first controlled optically. To reduce the inhomogeneity of the cleaved surface that may present rough or flat and shining areas next to each other, only small crystals of few square millimeters were analyzed.

ARUPS and LEED measurements were done in a VSW-ESCA lab, equipped with a HAC 5000 hemispherical analyzer, a standard He lamp and an Omicron back scattering LEED. STM experiments were performed with an Omicron VT-UHV-STM. All reported results were obtained at room temperature, in a base pressure of $5 \cdot 10^{-10}$ mbar.

3. RESULTS AND DISCUSSION

The clean surface of $P_4W_8O_{32}$ obtained by cleavage in UHV is characterized by a weak conduction band, detectable on the energy distribution curve (EDC) recorded at normal emission and using He II radiation (Fig.1). The conduction band has a bandwidth of about 0.8 eV and is well separated from a valence band by a depleted region of about 2 eV. The low intensity of this depleted region reflects the cleanliness and the good crystalinity of the surface, since both a surface contamination and a surface degradation produced by an Ar^+ ion etching have been found to increase the density of states in this region. The conduction band exhibits several structures, more evidenced by He I UPS or PES, that has lead to the determination of the experimental band structure [8]. The valence band also shows resolved structures around its maximum, that expresses the octahedral symmetry of the oxygen sites around the tungsten atoms. The double structure located at 10.6 and 11.8 eV, that is absent of the EDC curve of the pure tungsten oxides, is a doublet reflecting the P 3p shallow core level. The position of this core level clearly shows that the phosphorus atoms contribute not to the conduction band, but to the t2g bonding level. Thus, the valence band is mainly filled by oxygen type electrons. On the other hand, the conduction band is filled by electrons with the transition metal character, as evidenced by resonant photoemission in the parent compound η-Mo_4O_{11} [7]. Consequently one should expect that scanning the surface of $P_4W_8O_{32}$ with an energy up to 2 eV would image essentially the tungsten states. Nevertheless, several authors predict

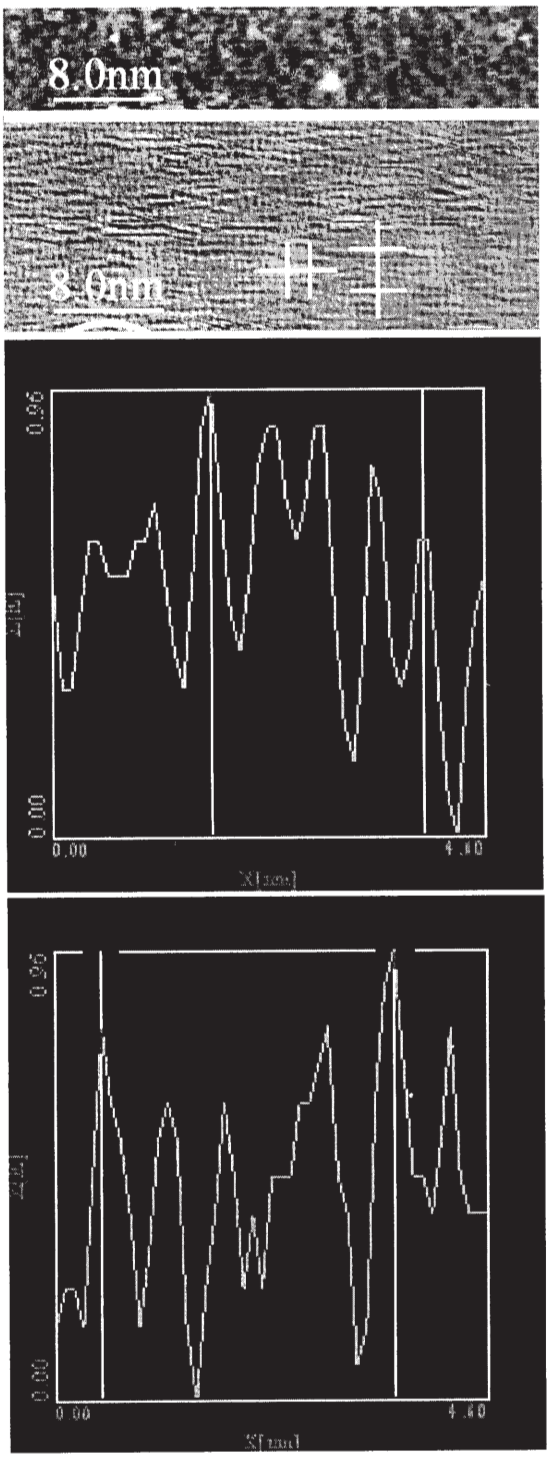

Fig 3. STM image of the (001) surface: A] image of a relaxed (001) facet; B] Filtered image obtained by fast Fourier transform (FFT) C] horizontal (H) and vertical (V) profiles revealing a 5.6 Å x 6.0 Å rectangular modulation.

in the parent sodium tungsten bronzes an oxygen contribution to the conduction band states higher than 15% [10].

After the cleavage a (001) surface, the crystalline quality of the remaining sample has been controlled by low energy electron diffraction at 49 eV (Fig. 2). The surface appears to be very sensitive to the electron bombardment, and the pattern disappears briefly after one minute of exposure. The surface has a LEED pattern characteristic from the (001) plane. It reveals a long distance order over the whole crystal, and a rectangular periodic pattern. In the two perpendicular directions, the ratio of the distances between the Bragg spots is about 1.25, that is very close to the ratio of the bulk parameters, a^*/b^* = 1.245. The untreated cleaved surface appears as a simple (1x1) (001) surface, without any surface reconstruction at long distance range.

STM images have been recorded in topographic mode on two samples cleaved in UHV, using a tip bias voltage ranging from +0.8 up to +2 V. The tunnel current of 0.5 nA was kept constant and a calibration was done on copper plate. The samples exhibit flat surfaces of few microns, with a very low corogation. A first type of STM image was obtained on both samples (Fig. 3a) The fast Fourier transform of a type I image reveals a rectangular periodicity, with parameters 5.6 E by 6.0 E, as they are extracted from the horizontal and vertical profiles (Fig. 3c).

These type I parameters appear very close to the bulk parameters of the (001) plane (a = 5.29 Å, b = 6.57 Å), and one can simply attribute the type I image to a relaxed (001) facet. Such an image, that is unchanged when the bias voltage is reduced to +0.8 V, value of the conduction bandwidth, results from the tunneling of the conduction electrons, which have a W character. It reflects principally the array of the WO_6 octahedra in the infinite octahedra slabs, rather than the lattice of the PO_4 tetrahedra in the planes (Fig. 4). The PO_4 planes act as an insulating barrier between the STM tip and the conducting electrons confined in the octahedra slabs.

Without any treatment, the top surface appears to be a relaxed (1 x 1) surface, with a smaller in plane anisotropy. $P_4W_8O_{32}$ has a layered orthorhombic structure that can be described as a stacking of tilted WO_6 octahedra slabs connected by a double plane of PO_4 tetrahedra. In the slabs, the WO_6 octahedra are ordered with a distorted perovskite structure. Two successive octahedra slabs are alternate, reflecting each other in mirror symmetry. The $(001)_p$ perovskite plane [the index p refers to the perovskite

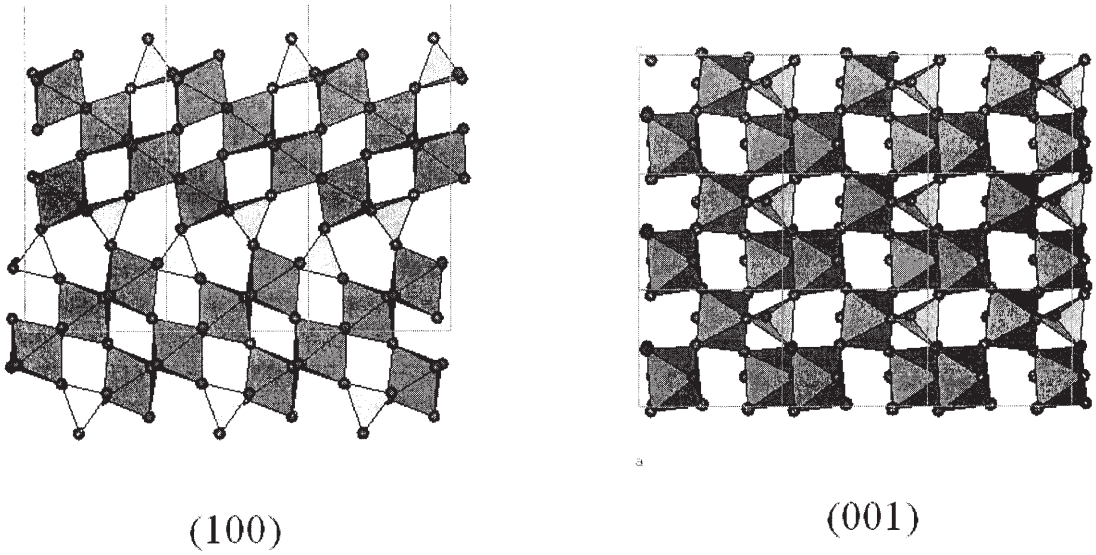

Fig. 4. Crystallographic structure of the $P_4W_8O_{32}$ bronze projected on the [100] and [001] planes. Anions are located at the center of the PO_4 tetrahedra and of the WO_6 octahedra, that share corners. The PO_4 tetrahedra delimit the infinite slabs of WO_6, built with 4 octahedra chains.

structure] is tilted alternatively by an angle of ± 35 with respect to the (001) orthorhombic plane. Based on this description, our results are consistent with a bulk truncation in the vicinity of the PO_4 planes. The disappearance of the alternate upper slab allows a relaxation that tends to restore the square symmetry of the remaining WO_6 slab.

Fig. 5 shows the STM image of a natural surface with a 17.6 Å x 6.05 Å periodic structure. This surface looks like a (3 x 1) reconstruction of the precedent surface, with a triple parameter along the [100] direction. This reconstruction differs from the surface reconstructions detected in the parent tungsten bronze, Na_xWO_3 that has been intensively studied by STM imaging and theoretically modelised [10-12]. In fact, this (3x1) reconstruction concerns an untreated surface and not a thermodynamically stable surface, obtained after etching and post annealing in presence of oxygen, as reported in the literature. In addition, this (3x1) (001) surface differs from the Na_xWO_3 surfaces due to the presence of PO_4 tetrahedra. The (3x1) periodic structure may be generated by a periodic defect of the (001) facet, for intense a periodic lack of PO_4 tetrahedra, as shown on the Fig. 6. Since the tetrahedra are aligned on lines parallel to the [010] direction, a bulk truncation removing every third line of PO_4 tetrahedra, will give a tripling of the surface parameter in the [100] direction.

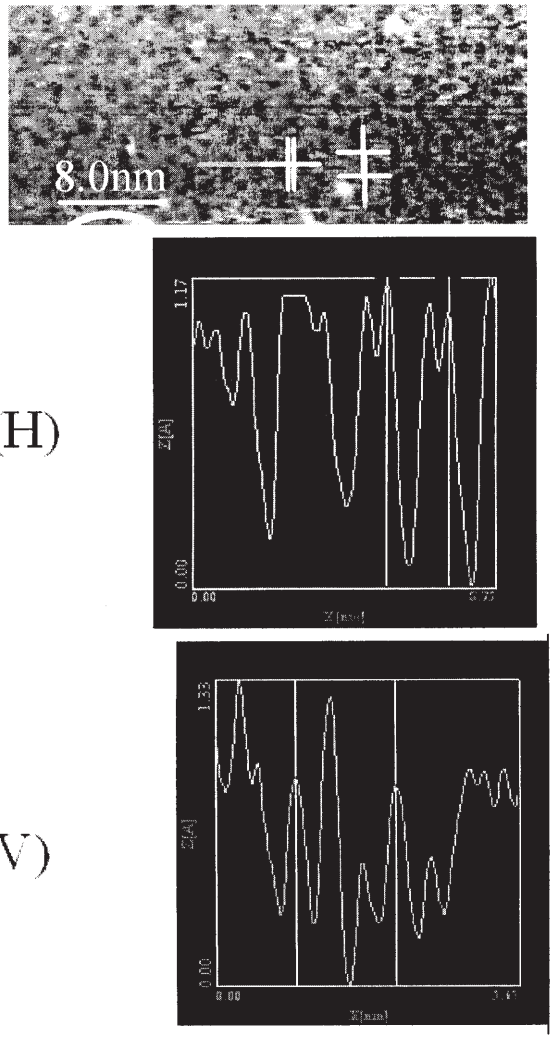

Fig. 5. STM image of a (001) surface and its horizontal (H) and vertical (V) profiles: the 17.8 Å x 6.0 Å modulation reveals a (3x1) reconstruction of the (001) facet.

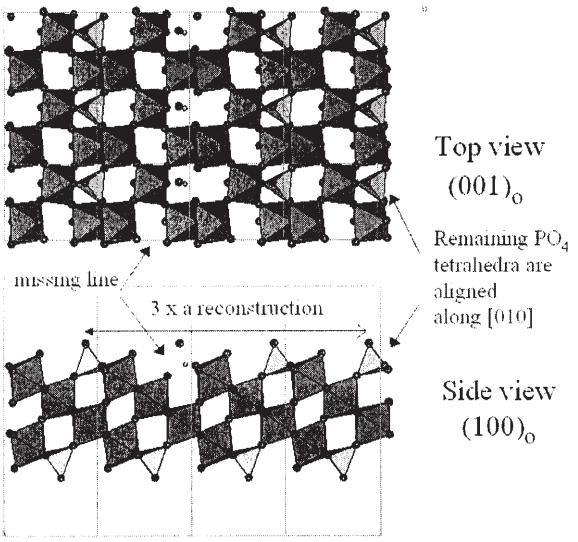

Fig. 6. Hypothetical (3x1) reconstruction of the (001) facet induced by an ordered surface defect: one line of PO_4 tetrahedra every three lines is removed.

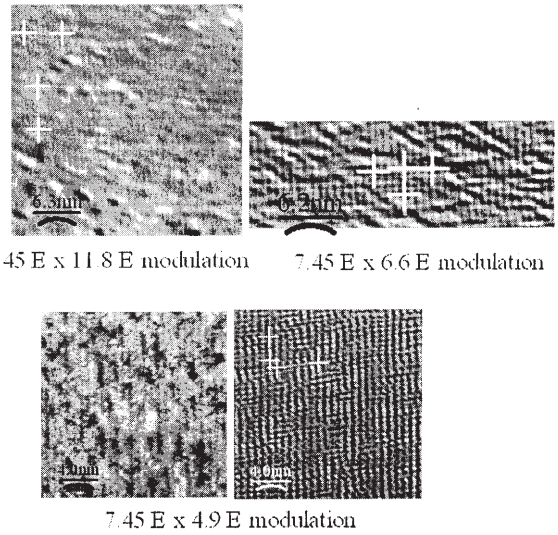

Fig. 7. Direct or filtered STM images showing 7.45 Å x 11.8 Å, 7.45 Å x 6.6 Å and 7.45 Å x 4.9 Å rectangular modulations. They are related to the perovskite $(001)_p$ plane of the octahedra slabs and correspond to $(001)_p$ facets.

Imaging (001) cleaved surfaces may also reveal facets with periodic structures like 7.45 Å x 11.8 Å, 7.45 Å x 4.9 Å or 7.45 Å x 6.6 Å (Fig. 7). The 7.45 Å distance seems to play a key role on these facets of type II, as well as the distance of 11.8 Å. 7.45 Å corresponds to the distance between second neighboring W sites, along the W1-W2-W2- W1 chains, while 11.8 Å corresponds approximately to the W1- -W1 distance along this chain (Fig. 8). These remarks allow to correlate these surfaces of type II directly to the WO_6 slabs and should reflect the perovskite structure of the slabs. If the bulk truncation removes all the PO_4 tetrahedra from the top of a WO_6 slab, the remaining surface may be described as a stepped $(001)_p$ perovskite surface tilted by 35° (Fig. 8). The STM images of type II reflect thus $(001)_p$ facets that correspond to the densest planes of the structure.

As shown in Fig. 8, each $(001)_p$ plane is ended by a step parallel to [010] of the orthorhombic structure. In the $[100]_p$ direction, parallel to the W1-W2-W2- W1 chains, the width of the step corresponds

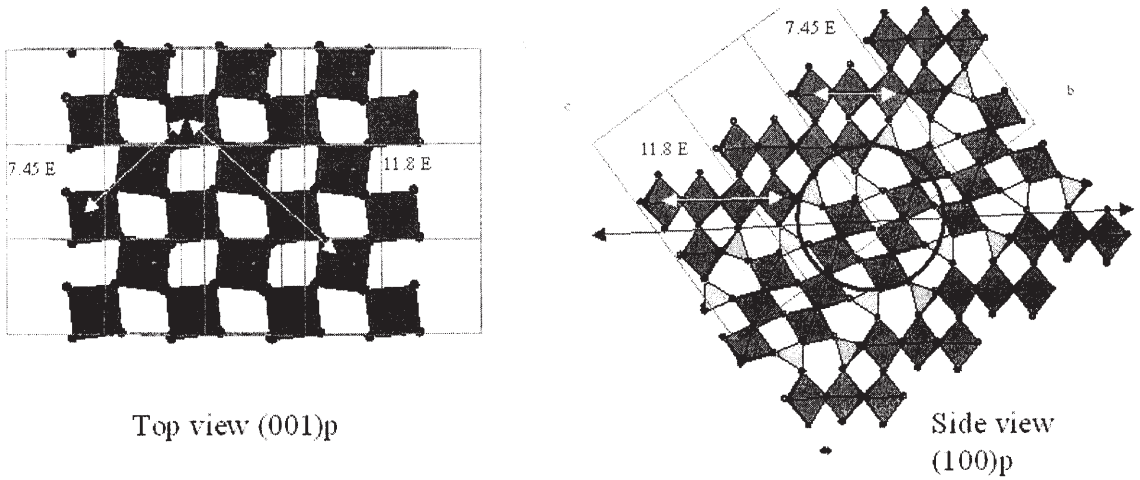

Fig. 8. Structure of the octahedra slabs with perovskite symmetry and possible truncation parallel to the $(001)_p$ plane. The open circle indicates the zone where the cleavage plane crosses the alternate slab. Characteristics of the steps and some interatomic distances are shown.

to two WO_6 octahedra that is about the measured 7.45 Å parameter. Perpendicularly, the 11.8 Å distance is related to the W-W-W-W chain, but it also corresponds to the width of the alternate neighboring slab. This second slab, tilted by about 70 from the first one, can also be truncated in the same plane. Nevertheless, the truncation of the alternate slab induces some defects due to the breaking of the W-W-W-W chain or to the appearance of W-W-P short chains. Such defects may also appear in direct slab, and originate very likely the 4.9 Å and 6.6 Å parameters that have been occasionally detected.

Many of the periodic structures detected on the (001) or on the $(001)_p$ facets result from the surface defects. Post treatments like annealing in oxygen should reduce the number and the size of the defects and stabilize the facets. Nevertheless, one should wonder if such treatments would be suitable for the observation of the charge density wave, that is the most important property of $P_4W_8O_{32}$. It is well known that any defect will act again the creation of the charge density wave by shorting the coherence length of the CDW. But it was proved experimentally that cleaved surfaces are good enough for imaging the CDW, at least in the molybdenum oxide and bronzes [13]. The detection of the CDW in $P_4W_8O_{32}$ should be probably possible, but the selection of (001) facets would be necessary, since the CDW extends in the (001) plane.

4. CONCLUSION

The cleavage of single crystal of P4W8O32 in UHV is the relevant way to determine experimentally the electronic structure of this tungsten bronze, free of surface contamination. The metallic character of this oxide is confirmed by the appearance of a weak conduction band, well separated from a large valence band, as in many tungsten bronzes. The long range order of a single crystal surface cleaved parallel to the (001) plane is controlled by low energy electron diffraction. This characterization nevertheless modifies rapidly the surface, making the LEED pattern vanishing and creating new states in the depleted region below the conduction band.

The local study at nanoscale range of the cleaved (001) surface reveals many situations, that correspond to two types of facets, the $(001)_o$ facets or $(001)_p$ facets [o and p refer respectively to the orthorhombic structure and to the perovskite structure of the WO_6 slabs]. These facets can be well crystallized or affected by surface defects. They are responsible for some reconstructions, like a (3x1) $(001)_o$ surface, or reveal the presence of distorted regions, like that ones corresponding to the alternated slabs.

ACKNOWLEDGEMENTS

The authors are very grateful to Dr O. Perez (Crismat-CNRS, Caen, France) for providing us with single crystals.

REFERENCES

[1] P. Roussel, O. Pérez and Ph. Labbé // *Acta Cryst.* **B57** (2001) 603.

[2] P. Foury-Leylekian, E. Sandré, S. Ravy, J.-P. Pouget, E. Elkaim, P. Roussel, D. Groult and Ph. Labbé // *Phys. Rev. B* **66**.(2002) 075116.

[3] J. A. Jobst, S. Geupel and S. van Smaalen // *Phys. Rev. B* **64** (2001) 104105.

[4] C. Schlenker, C. Hess, C. Le Touze and J. Dumas // *J. Phys. I France* **6** (1996) 2061; J. Dumas, U. Beierlein, S. Drouard, C. Hess, D. Groult, Ph. Labbé, P. Roussel, G. Bonfait, E.Gomez Marin and C. Schlenker // *J. Solid State Chem.* **147**(1999) 320.

[5] U. Beierlein, C. Hess, C. Schlenker, J. Dumas, R. Buder, D. Groult, E. Steep, D. Vignolles and G. Bonfait // *Eur. Phys. J. B* **17** (2000) 215.

[6] S. Drouard, D. Groult, J. Dumas, R. Buder and C. Schlenker // *Eur. Phys. J. B* **16** (2000) 593.

[7] H. Guyot, N. Motta, J. Marcus, S. Drouard and H. Balaska // *Surf. Science* **482-485** (2001) 759.

[8] A. Mascaraque, L. Roca, J. Avila, S. Drouard, H. Guyot and M. C. Asensio // *Phys. Rev. B* **66** (2002) 115104.

[9] L. Roca, A Mascaraque, J. Avila, S. Drouard, H. Guyot and M.C. Asensio // *Phys. Rev. B* **69** (2004) 75114.

[10] T. Parker, P. Wincott, A. Munz, T. Bertrams, G. Thornton, S.C. Parker, P.M. Oliver, R. Dixon, F.H. Jones, T. Fishlock and R.G. Egdell // *Surf. Sci.* **424** (1999) 177.

[11] F.H. Jones, K. Rawlings, S. Paker, J.S. Foord, P.A. Cox, R.G. Egdell and J.B. Pethica // *Surf. Sci.* **336** (1995) 181.

[12] F.H. Jones, K. Rawlings, R.A. Dixon, T.W. Fishlock and R.G. Egdell // *Surf. Sci.* **460** (2000) 277.

[13] P. Mallet, K. M. Zimmermann, Ph. Chevalier, J. Marcus, J. Y. Veuillen and J. M. Gomez Rodriguez // *Phys. Rev. B* **60** (1999) 2122; P. Mallet, H. Guyot, J. Y. Veuillen and N. Motta // *Phys. Rev. B* **63** (2001) 165428.